Talanta 115 (2013) 214–221

Contents lists available at ScienceDirect

Talanta

journal homepage: www.elsevier.com/locate/talanta

Gold nanoparticle-modified graphite pencil electrode for the high-sensitivity detection of hydrazine

Md. Abdul Aziz [a], Abdel-Nasser Kawde [a,b,*]

[a] Chemistry Department, King Fahd University of Petroleum and Minerals, Dhahran 31261, Saudi Arabia
[b] Chemistry Department, Faculty of Science, Assiut University, Assiut 71516, Egypt

ARTICLE INFO

Article history:
Received 27 February 2013
Received in revised form
16 April 2013
Accepted 17 April 2013
Available online 2 May 2013

Keywords:
Gold nanoparticles
Graphite pencil electrode
Hydrazine
Square wave voltammetry
Sensor

ABSTRACT

A novel gold nanoparticle-modified graphite pencil electrode (AuNP-GPE) is prepared just by immersing a bare GPE in AuNP solution, followed by heating for 15 min. The bare and modified GPEs are characterized by FE-SEM imaging and cyclic voltammetry. The AuNP-GPEs showed excellent electrocatalytic activities with respect to hydrazine oxidation, with good reproducibility. To reduce the quantification and detection limits, and increase the hydrazine sensitivity, the pH and square wave voltammetry parameters are optimized. A square wave voltammetry study as a function of the hydrazine concentration showed that the AuNP-GPE detector's quantification limit was 100 nmol L^{-1} hydrazine, much lower than the value obtained using amperometry (10 μmol L^{-1}). The limits of detection (at 3σ) for hydrazine sensing at AuNP-GPEs using square wave voltammetry and amperometry were 42 nmol L^{-1} and 3.07 μmol L^{-1}. Finally, the modified electrode was used to determine the hydrazine concentration in drinking water, and satisfactory results are obtained. This simple, rapid, low-cost method for fabricating a modified electrode is an attractive approach to the development of new sensors.

© 2013 Elsevier B.V. All rights reserved.

1. Introduction

Hydrazine (H_2N-NH_2) is a small inorganic molecule with a molecular weight of 32 g/mol. It is a water-soluble volatile colorless liquid [1]. Hydrazine is used in certain rockets and spacecraft, for example, as fuel in space shuttles. It is also used as a pesticide in agriculture, an intermediate in pharmaceuticals and as a corrosion control additive in the treatment of water boilers [1,2]. Hydrazine is a starting material for the production of other materials, such as farm chemicals and plastic foams [1,2]. The widespread use of hydrazine has, unfortunately, afforded many opportunities for contaminating the environment. Hydrazine is toxic and easily absorbed by oral, dermal or inhalation routes of exposure [1,2]. The lungs, liver, kidney, and central nervous systems of living organisms can be injured if hydrazine is inhaled or introduced to the skin [1,2]. Serious effects on the reproductive system are observed in animals after hydrazine inhalation [1]. These effects have included reduced ovary and testes size and decreased sperm production [1]. Hydrazine has also been identified as a carcinogenic agent [1,3]. Therefore, the development of a simple, inexpensive, accurate, and reliable method for the routine analysis of hydrazine is extremely beneficial.

Among the conventional analytical methods [4,5], electroanalytical methods have attracted attention due to their simplicity, portability, selectivity, sensitivity, moderate cost, and amenability to miniaturization [6–8]. Gold (Au), platinum (Pt), glassy carbon (GC), and indium tin oxide (ITO) electrodes are commonly used as working electrodes in electroanalytical tools; however, the high cost or low signal-to-noise ratio impose a barrier to the use of these electrodes in sensitive routine analysis instruments. The material of the graphite pencil electrodes (GPEs) is low in cost, easily maintained, displays strong adsorption properties and a low background current, and good electrocatalytic properties toward some electroactive molecules, and displays a wide potential window [8–14]. On the other hand, GPEs exhibit poor electrocatalytic sensitivity toward diverse electroactive molecules, such as dopamine and sulfide [15,16]. As a result, the modification of GPEs, using a suitable electrocatalyst, is crucial to the fabrication of sensitive electrochemical sensors.

Interestingly, nanomaterials are used in a variety of electrocatalyst applications because they exhibit good electrocatalytic properties, a high surface-to-volume ratio, a high stability, they are widely available, and they provide fast electron transfer rates. Various electrodes were utilized in the electrochemical detection of hydrazine, for example, Au nanoparticles (AuNPs) on ZnO-multiwall carbon nanotube (MWCNT) film-modified glassy carbon electrodes (GCEs) [17], AuNPs on choline film-modified GCEs [18], PdNPs on MWCNT- and Nafion-modified GCEs [19], PdNPs- and poly(2-acryalamido-2-methyl-propane-sulfonic acid)-doped

* Corresponding author at: Chemistry Department, King Fahd University of Petroleum and Minerals, Dhahran 31261, Saudi Arabia. Tel.: +966 13 860 2145; fax: +966 13 860 4277.
E-mail addresses: ncaug11@gmail.com, akawde@kfupm.edu.sa (A.-N. Kawde).

0039-9140/$ - see front matter © 2013 Elsevier B.V. All rights reserved.
http://dx.doi.org/10.1016/j.talanta.2013.04.038

polyaniline layer-modified GCEs [20], composite films of AuNPs and MWCNTs on GCEs [21], AuNP–polypyrrole nanowire-modified GCEs [22], Nano-copper oxide-modified GCEs [23], nickel hexacyanoferrate NP-modified carbon ceramic electrodes [24] AuNP- and thiolated DNA-modified Au electrodes [25], α-Fe_2O_3 NP-modified Au electrodes [26], zinc oxide Nano rod electrodes [27] and nanoporous gold NP-modified indium tin oxide electrode [28]. AuNPs have also shown good electrocatalytic properties toward other electroactive molecules, including hydrazine, norepinephrine, *p*-aminophenol, acetaminophen and atenolol [17,18,29–32].

The long-term advantage of nanomaterial-based electrochemical sensors depends somewhat on simplicity and reproducibility of the method used to immobilize or prepare the NPs on electrode surfaces. Nanomaterials may be immobilized or prepared on GPE surfaces via

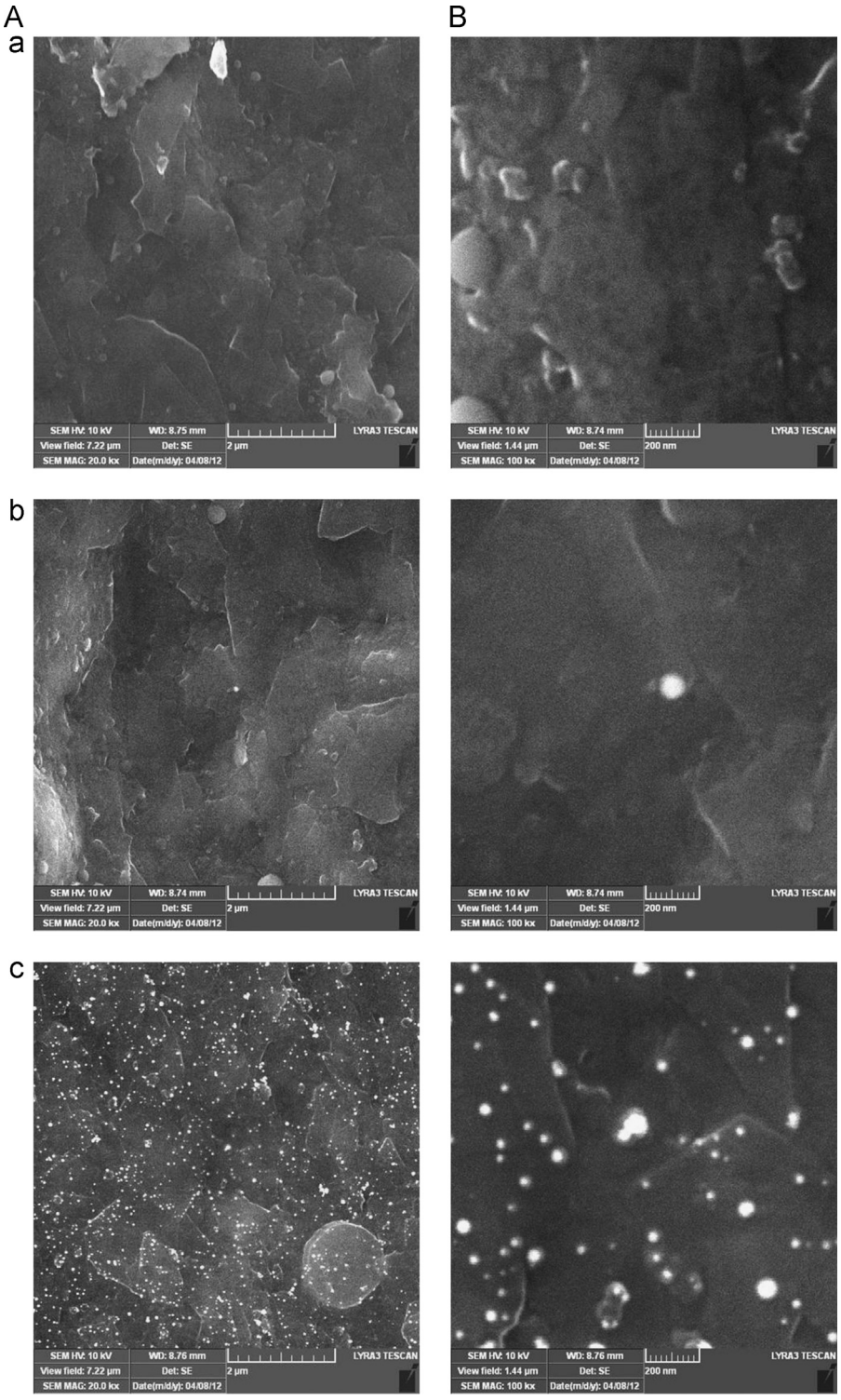

Fig. 1. FE-SEM images at two different magnifications, 2 μm (A) and 200 nm (B), of bare (a) and AuNP-modified GPEs prepared by immersing the bare GPE in a AuNPs solution at RT (b) or at 75 °C (c) for 15 min.

various techniques, including chemical vapor deposition [33], electrochemical deposition from a metal precursor [34–37], or electrochemical deposition from polymer-attached NPs [38,39]. Chemical vapor deposition and electrochemical deposition techniques are fast processes and, therefore, produce poorly reproducible results. Moreover, these methods require sophisticated instruments and trained technicians, both of which factors increase the overall production cost. Alternative comparatively uncomplicated methods of chemically attaching the nanomaterials onto a solid substrate via cross-linking molecules are widely used [40,41]; however, such methods require long times, are multistep processes, and the linking molecules can affect the electron transfer reactions. To overcome the limitations of the methods discussed above, a heat treatment method for preparing AuNPs attached to GPEs using an aqueous solution of $HAuCl_4$ and ascorbic acid is proposed. This technique requires only short periods of time and does not require the use of cross-linking molecules. To the best of authors knowledge, no previous reports have described preparation methods that depend directly on the attachment of pre-synthesized AuNPs onto GPE surfaces.

This manuscript describes an easy and innovative method for attaching AuNPs directly onto GPEs to obtain AuNP-modified GPEs. The prepared modified electrodes are low in cost, disposable, renewable, highly reproducible and demonstrate good electrocatalytic properties and a high selectivity for hydrazine.

2. Materials and methods

2.1. Reagents

Hydrogen tetrachloroaurate(III)hydrate, L-ascorbic acid (AA), and 3,4-dichlorophenol were received from Sigma-Aldrich (http://www.sigmaaldrich.com/united-states.html). Phenol and disodium hydrogen phosphate were obtained from Fluka (http://www.sigmaaldrich.com/united-states.html). Hydrazine hydrate was supplied by BDH Chemical Ltd. (Poole, England). Sodium dihydrogen phosphate was supplied by Fisher Scientific Company (http://www.fisherscientific.com/). Hi-polymer graphite pencil HB black leads were obtained from Pentel Co. LTD. (Japan). All leads had a total length of 60 mm and a diameter of 0.5 mm, and were used as received. Deionized water with a resistivity of 18.6 $M\Omega\,cm^{-1}$ is used to prepare all solutions. The water is obtained directly from a PURELAB® Ultra Laboratory Water Purification System (http://www.water.siemens.com/en/products/laboratory_water/water_purification_systems/Pages/PURELAB_Ultra_Laboratory_Water_Purification_System.aspx).

2.2. Apparatus and procedures

A Jedo mechanical pencil (Korea) is used as a holder for both the bare and AuNP-modified graphite pencil leads. Electrical contact with the lead was achieved by soldering a copper wire to the metallic parts that held the lead in place inside the pencil. The pencil was fixed vertically such that 15 mm of the pencil lead was extruded from the holder. A 10 mm stretch of the lead was immersed in the solution. This length corresponded to a geometric electrode area of 15.90 mm^2. The pencil electrode has been described in detail before [42]. A CHI 660 (http://www.chinstruments.com/) was used for all electrochemical experiments. The electrochemical cell contained a bare or AuNP-modified GPE as a working electrode, a Pt wire counter electrode, and Ag/AgCl (sat. KCl) reference electrode. FE-SEM images of the electrodes were recorded using a TESCAN LYRA 3 (http://www.tescan-usa.com/products/lyra3-gm.htm) at the Center of Research Excellence in Nanotechnology (CENT), King Fahd University of Petroleum and Minerals (KFUPM), Kingdom of Saudi Arabia.

2.3. Gold nanoparticle-modified graphite pencil electrode preparation

Equal volumes (1.5 mL of each aqueous solution) containing 1.65 mmol L^{-1} AA and 1.0 mmol L^{-1} gold(III) chloride were mixed using a pipette at room temperature (RT) in a 3.0 mL test tube to form AuNPs [43]. To obtain the AuNP-modified GPE, a bare GPE is immersed for 15 min into a test tube placed in a 75 °C water bath. The AuNP-modified GPE was removed and washed by gentle dipping two times into deionized water. The AuNP-modified GPE was then dried at 60 °C for 5 min prior to use. This method for preparing the AuNP-modified GPEs was used throughout the studies reported here, unless otherwise stated.

3. Results and discussion

3.1. Morphological characterization and electrochemical investigation

Prior to modifying the GPE surfaces, the AuNPs were synthesized in 3 mL test tubes simply by reducing Au^{3+} ions in the presence of AA according to previous reports [43]. A bare GPE was then immersed in the test tube and incubated at RT or 75 °C for 15 min to prepare a AuNP-modified GPE. FE-SEM images of the bare and AuNP-modified GPEs were then recorded at different degrees of magnification (Fig. 1A and B). Fig. 1a–c shows FE-SEM images of a bare GPE, a AuNP-modified GPE at RT, or a AuNP-modified GPE at 75 °C, respectively. Comparison of Fig. 1a–c clearly shows that the AuNPs minimally attached to the GPE surfaces under RT treatment, whereas the AuNPs were efficiently attached upon incubation at 75 °C. The AuNP-modified GPE, which was prepared by heating at 75 °C, is denoted as 'AuNP-GPE' in the remainder of this discussion. The sizes of the AuNPs on a GPE fell in the range 20–85 nm (Fig. 1Bc). A low-magnification view of the AuNP-GPE (Fig. 1Ac) confirmed the presence of a homogeneous distribution of AuNPs on the GPE surface.

To confirm the existence of AuNP on the GPEs, cyclic voltammograms (CVs) of a bare GPE (Fig. 2a) and a AuNP-GPE (Fig. 2b) were recorded in 0.1 mol L^{-1} NaOH. The CV of the AuNP-GPE showed higher anodic and cathodic currents than the CV of the bare GPE. Moreover, the cathodic peak at 0.119 V was only present in the CV of the AuNP-GPE. Overall, only the CV of the AuNP-GPE displayed a redox signal characteristic of gold [31,44]. The CV experiments confirmed the presence of Au on AuNP-GPE.

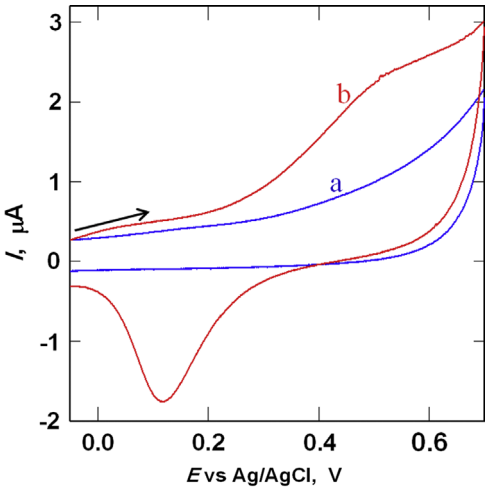

Fig. 2. CVs in a 0.1 mol L^{-1} NaOH aqueous solution at a bare GPE (a) and at a AuNP-GPE (b). Scan rate: 100 mV s^{-1}. Fig. 1c conditions were used here to prepare the AuNP-GPE.

However the mechanism of the AuNP-GPE binding is not entirely known yet, it is well known that the AuNP (aq.) synthesized using AA is stabilized electrostatically due to the negative charge of the adsorbed excess of ascorbic acid (AA) on AuNPs [43]. It is also reported that the AuNP (aq.) synthesized at a temperature more than 55 °C by ascorbic acid is unstable [43]. Besides, Lopez-Sanchez et al. reported that weakly adsorbed stabilizing water soluble molecules can be removed by hot water extraction [45]. Hence, almost all of the adsorbed AA molecules are removed from the AuNP surface by the hot extraction at 75 °C. The binding between the almost bare AuNP and GPE might be physical adsorption.

3.2. Electrocatalytic oxidation of hydrazine

The electrocatalytic performances of bare GPE and AuNP-GPE are evaluated by recording the CVs in PB (0.1 mol L^{-1}, pH 7) in the absence (Fig. 3A) or the presence of 0.5 mmol L^{-1} hydrazine (Fig. 3B). The anodic current of the AuNP-GPE (Fig. 3Ab) in 0.1 mol L^{-1} PB (pH 7.0) was slightly higher with an oxidation peak than the anodic current of the bare GPE (Fig. 3Aa). The higher background current in the anodic scan is due to the AuNPs oxidation [46], which behave differently from the bulk gold electrode. At the bare GPE (Fig. 3Ba), hydrazine did not oxidize at potentials < 0.4 V and did not show any oxidation peaks over the entire potential window tested. Thus, the bare GPE requires an overpotential to achieve the electrooxidation of hydrazine. On the other hand, hydrazine oxidation in the presence of the AuNP-GPE occurred near the starting potential during CV recording (Fig. 3Bb), and the oxidation peak appeared at +0.28 V. The oxidation current of hydrazine at the AuNP-GPE was much higher than that obtained at the bare GPE. These experiments clearly indicated that the presence of AuNPs on the GPE enhanced the signal and reduced the overpotential for hydrazine electrooxidation, both of which effects are essential for a sensitive and selective electrochemical hydrazine sensor.

3.3. Reproducibility

The reproducibility of the AuNP-GPE performance is verified by recording the CVs of a 0.5 mmol L^{-1} hydrazine in the presence of a series of newly modified electrode surfaces (data not shown). The intraday experiments showed a peak current of 54.1 ± 3.3 μA (mean ± standard deviation) with an RSD of 6.0%, whereas the

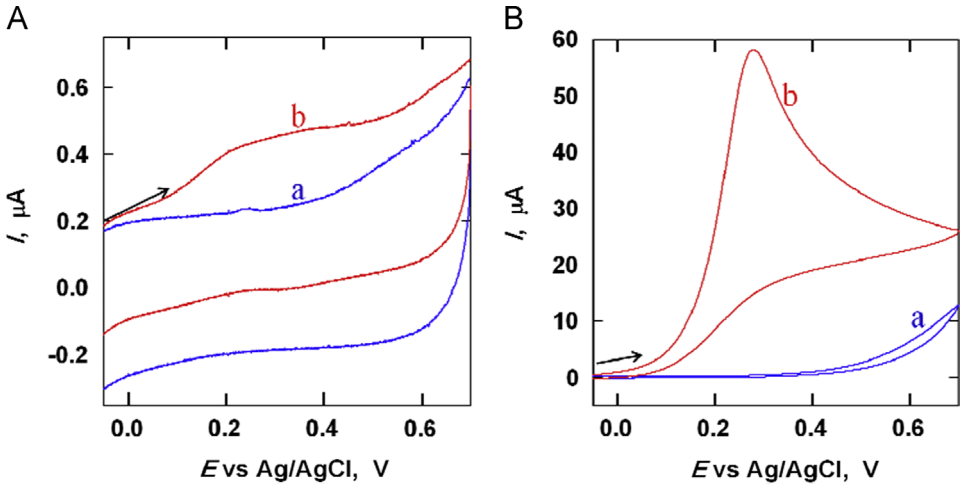

Fig. 3. CVs in 0.1 mol L^{-1} PBS (pH 7) in the absence (A) or presence (B) of 0.5 mmol L^{-1} hydrazine at a bare GPE (a) and at a AuNP-GPE (b). Scan rate: 100 mV s^{-1}. Fig. 1c conditions were used here to prepare the AuNP-GPE.

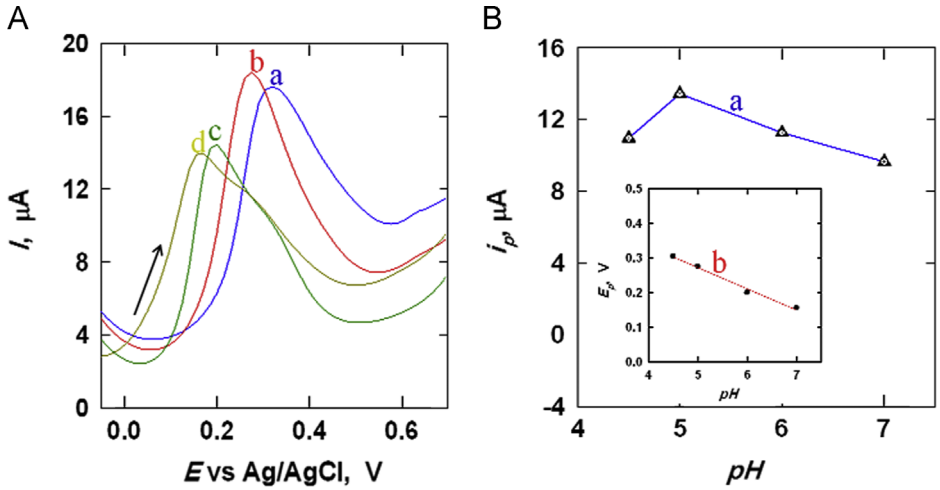

Fig. 4. (A) Square wave voltammograms of a 25 μmol L^{-1} hydrazine solution in 0.1 mol L^{-1} PB at various pH values: (a) pH 4.5, (b) pH 5.0, (c) pH 6.0, and (d) pH 7.0 at a AuNP-GPE. Working condition of the pulse width (increment), 15 mV; pulse height (amplitude), 100 mV; frequency, 30 Hz. (B) Plots of the pH vs. peak current (a) or peak potential (b). Fig. 1c conditions were used here to prepare the AuNP-GPE.

interday experiments showed a peak current of 56.9 ± 4.9 μA with an RSD of 8.77%, i.e., the AuNP-GPE preparation yielded reproducible electrode performances.

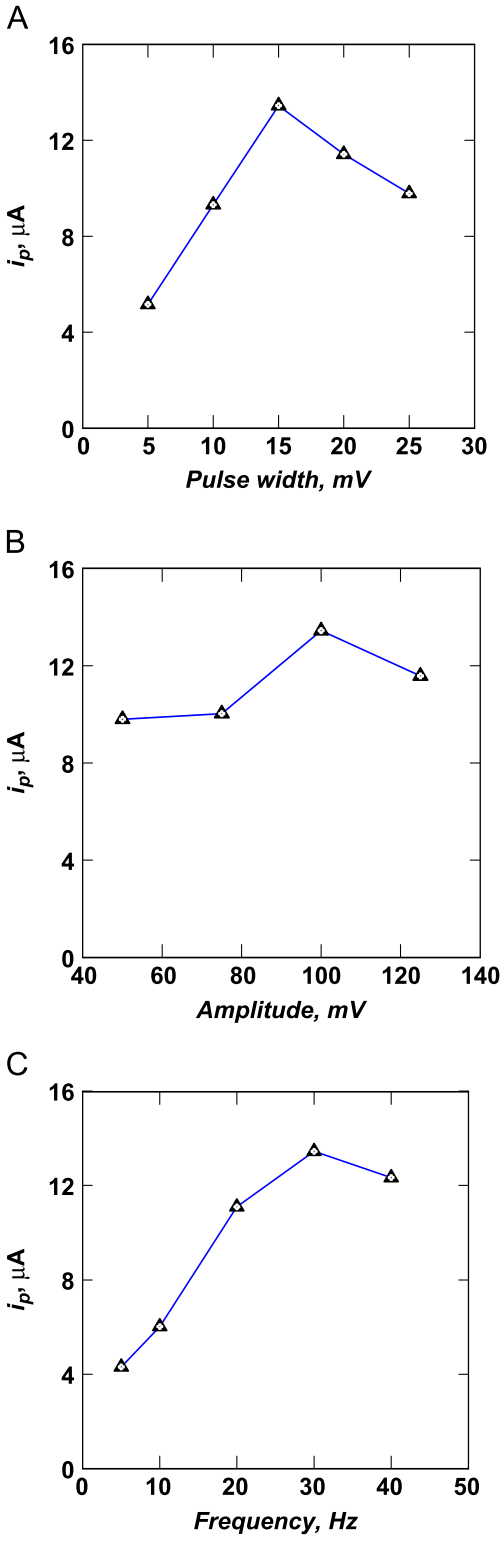

Fig. 5. Plots of the peak current vs. the pulse width (A), amplitude (B), or frequency (C) of the square wave voltammograms of a 25 μmol L^{-1} hydrazine solution at a AuNP-GPE. Fig. 1c conditions were used here to prepare the AuNP-GPE. The other working conditions were as in Fig. 4.

3.4. Parameter optimization for electroanalytical hydrazine determination

Although CV technique is widely used in electrochemical investigations, the background current is often a barrier to obtaining low detection limits in electroanalysis. Square wave voltammetry (SWV) yields a higher sensitivity and superior suppression of unwanted background currents; however, the sensitivity of SWV depends partially on the pH and the electroanalytical parameters [47]. Therefore, the pH effects and SWV parameters were examined in the context of hydrazine electrooxidation.

3.4.1. Effect of pH

The effect of pH on the SWV response to the electrooxidation of a 25 μmol L^{-1} hydrazine solution in PB at a AuNP-GPE was systematically studied over the pH range 4.5–7 (Fig. 4). As the pH increased, the electrooxidation peak potential (E_p) of hydrazine is linearly shifted toward less positive potentials with a slope of −61.5 mV per pH unit (Fig. 4Bb). This slope is remarkably close to the anticipated Nernstian slope of −59 mV for a four-electron, four-proton process. Therefore, the mechanism of the hydrazine oxidation at the AuNP-GPE could be expressed by Eq. (1), as reported previously [48,49]

$$N_2H_4 \rightarrow N_2 + 4H^+ + 4e^- \quad (1)$$

Fig. 4Ba shows a plot of the peak current for a 25 μmol L^{-1} hydrazine solution vs. pH. The curve clearly showed that a pH of 5.0 yielded the highest electrooxidation signal, with peak potential of +0.275 V. As a result, pH 5.0 is selected as the optimum pH for further experiments.

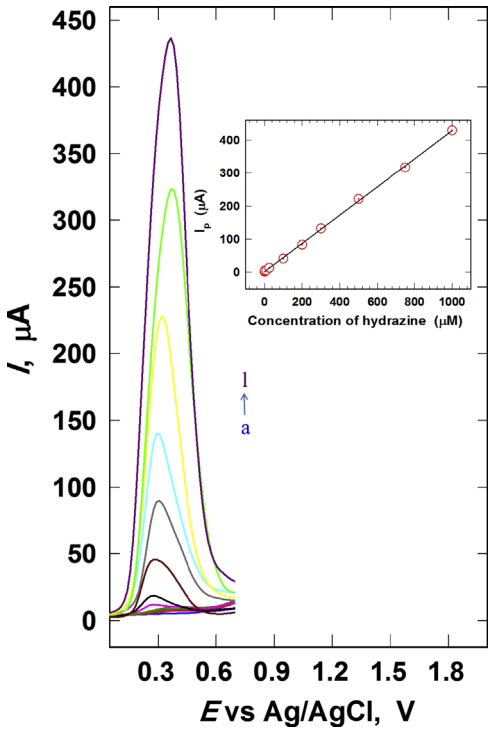

Fig. 6. Square wave voltammograms in PB (0.1 mol L^{-1}, pH 5.0) containing different μmol L^{-1} concentrations of hydrazine at a AuNP-GPE: (a) 0.0, (b) 0.05, (c) 0.1, (d) 1.0, (e) 10.0, (f) 25.0, (g) 100.0, (h) 200.0, (i) 300.0, (j) 500.0, (k) 750.0, and (l) 1000.0 μmol L^{-1} hydrazine. Fig. 1c conditions were used to prepare the AuNP-GPE. The other working conditions were as in Fig. 4. The inset shows the corresponding calibration curve.

3.4.2. Effects of SWV parameters

The effects of the pulse width (Fig. 5A), amplitude (Fig. 5B), and frequency (Fig. 5C) on the SWV signal for the electrooxidation of a 25 μmol L^{-1} hydrazine solution in PB (0.1 mol L^{-1}, pH 5) at the AuNP-GPE are examined (Fig. 5). The peak current indicated that 15 mV, 100 mV, and 30 Hz were the optimum pulse width, amplitude, and frequency, respectively.

3.5. Stability

The stability of the AuNP-GPE was tested by monitoring the peak current after five consecutive SWV recordings using a single AuNP-GPE in PB (0.1 mol L^{-1}, pH 5) containing 0.75 mmol L^{-1} hydrazine (data are not shown). The recorded peak current was found to decrease by only 5.0% of its initial value. This result indicated that the modified electrode was quite stable.

3.6. Square wave voltammetric determination of hydrazine concentration

Under optimum conditions, square wave voltammograms are recorded at the AuNP-GPE to determine the limits of quantification and detection of hydrazine. The calibration curve (inset of Fig. 6) was constructed from the signal, after subtracting the mean of the zero hydrazine response, for the concentration range between 0.05 and 1000 μmol L^{-1}. The calibration curve increases linearly as the hydrazine concentration increases and follows the linear regression equation $y=0.4260x+2.1864$ ($R^2=0.9995$). In all equations of this manuscript, x and y are noted as concentration of hydrazine and corresponding concentration dependence signal, respectively. The calculated limit of detection at 3σ was 42 nmol L^{-1} hydrazine. It should be noted that the net peak current of 50 nmol L^{-1} for hydrazine (1.9055 μA) is less than three standard deviations (SD) (2.2044 μA) of the signal obtained from the blank solution. However, the three standard deviations (SD) (2.2044 μA) of the signal obtained from the blank solution is less than the net peak current of 100 nmol L^{-1} hydrazine (3.0625 μA). The limit of quantification of the developed sensor is 100 nmol L^{-1} hydrazine. The obtained limits of quantification and detection for hydrazine sensing are much lower than that reported previously for other nanomaterial-modified carbon-based electrodes (Table 1).

3.7. Amperometric determination of hydrazine

The performance of the SWV method was compared with that of the amperometric method in the context of hydrazine detection

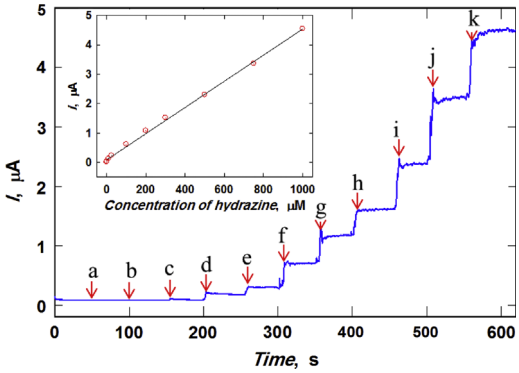

Fig. 7. Amperograms of the AuNP-GPE at 0.3 V in 10 mL 0.1 mol L^{-1} PBS (pH 5) upon the successive addition of hydrazine: (a) 0.05, (b) 0.10, (c) 0.9, (d) 9.0, (e)15, (f) 75, (g) 100, (h)100, (i) 200, (j) 250 and (k) 250 μmol L^{-1} hydrazine. Fig. 1c conditions were used to prepare the AuNP-GPE. The inset shows the calibration plots. The calibration curves were calculated by subtracting the current in the absence of hydrazine from the current at each concentration.

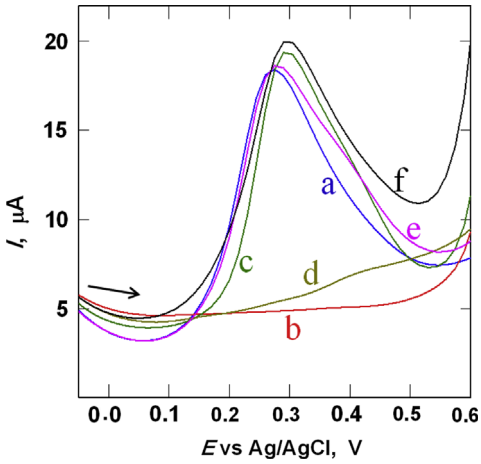

Fig. 8. Square wave voltammograms in 0.1 mol L^{-1} PB (pH 5) containing (a) 25 μmol L^{-1} hydrazine, (b) 100 μmol L^{-1} phenol, (c) 25 μmol L^{-1} hydrazine and 100 μmol L^{-1} phenol, (d) 100 μmol L^{-1} 3,4-dichlorophenol, (e) 25 μmol L^{-1} hydrazine and 100 μmol L^{-1} 3,4-dichlorophenol, and (f) 25 μmol L^{-1} hydrazine, 100 μmol L^{-1} phenol, and 100 μmol L^{-1} 3,4-dichlorophenol at a AuNP-GPE. Fig. 1c conditions were used to prepare the AuNP-GPE. Other working conditions were as in Fig. 4.

Table 1

Methods	Electrode	Sensing media (pH)	Limit of quantification (μmol L^{-1})	Limit of detection (μmol L^{-1})	Ref.
Differential pulse voltammetry (DPV)	PdNP/MWCNT-GCE	0.5 μmol L^{-1} H_2SO_4	2.5	1.0	19
DPV	AuNP/polypyrole nanowire-GCE	0.1 μmol L^{-1} PB (7.0)	1.0	0.20	22
DPV	Nickel hexacyanoferrate@TiO_2NPs-GCE	0.1 M PBS (8.0)	0.2	0.11	53
Amperometry	PdNP/polysulfonic acid-doped polyaniline-GCE	0.1 μmol L^{-1} PB (6.7)	40.0	0.42	20
Amperometry	ZnO nanoflower/MWCNTs-GCE	0.1 μmol L^{-1} PB (7.4)	0.6	0.18	50
a. CV b. Amperometry	PdNP/carbon black NP-GCE	0.5 μmol L^{-1} PB (9.0)	a. 10.0 b. 15.0	a. 8.80 b. 13.40	51
Amperometry	AuCuNPs/Graphene/ionic liquid-GCE	0.1 μmol L^{-1} PB (6.8)	0.2	0.10	52
Amperometry	4-(2(2-hydroxyphenylimino)methyl)benzene-1,2-diol/ MWCNT-GCE	0.1 μmol L^{-1} PB (7.0)	–	1.10	54
a. SWASV b. Amperometry	AuNP-GPE	0.1 μmol L^{-1} PB (5.0)	a. 0.1 b. 10.0	0.04 3.07	This work

Table 2

Sample	Added (μmol L^{-1})	Found (μmol L^{-1})	Recovery (%)
1	0.0	–	–
	10.0	9.87	98.70
	20.0	20.25	101.25
2	0.0	–	–
	20.0	19.82	99.14
	30.0	29.50	98.33

at the AuNP-GPE. Fig. 7 shows typical amperometric responses of the AuNP-GPE at +0.3 V upon successive additions of different concentrations of hydrazine. The hydrazine concentration at each spike was the same as the concentration used in the SWV concentration dependence study (Fig. 6). The 50 nmol L^{-1} and 100 nmol L^{-1} hydrazine solutions could not be detected using the amperometric method (Fig. 7a and b). The response current after subtracting the mean of the zero hydrazine response is linear with respect to the hydrazine concentration over the range 25–1000 μmol L^{-1} and follows the linear regression equation $y=0.0043x+0.1729$ ($R^2=0.9991$). Moreover, the calibration curve at the low concentration range (0.05–25 μmol L^{-1}; data not shown) shows a linear signal response with a higher sensitivity, and follows the linear regression equation $y=0.009x+0.0194$ ($R^2=0.9861$). The calculated limit of detection at 3σ was 3.07 μmol L^{-1} hydrazine. It should be noted that three SDs of the amperometric signal of blank solution (0.0471 μA) exceed the net amperometric signal of a 1 μmol L^{-1} hydrazine solution (0.0328 μA), yet is less than that of a 10 μmol L^{-1} hydrazine solution (0.1276 μA). The quantification limit of the developed sensor using the amperometry method is 10 μmol L^{-1} hydrazine. These limits of quantification (10 μmol L^{-1}) and detection (3.07 μmol L^{-1}) are much higher than the limits of quantification (100 nmol L^{-1}) and detection (42 nmol L^{-1}) obtained using the SWV method.

3.8. Interference

Phenolic compounds (e.g., phenol and 3,4-dichlorophenol), which are commonly present as hazardous materials in the environment, can potentially interfere with the hydrazine signal; therefore, the interference effects of a 25 μmol L^{-1} hydrazine solution in the presence of phenolic compounds were investigated (Fig. 8). The SWVs at AuNP-GPE in a PB solution (0.1 mol L^{-1}, pH 5) were recorded in the presence of 25 μmol L^{-1} hydrazine (Fig. 8a) and 100 μmol L^{-1} phenol (Fig. 8b), 25 μmol L^{-1} hydrazine and 100 μmol L^{-1} phenol (Fig. 8c), 100 μmol L^{-1} 3,4-dichlorophenol (Fig. 8d), 25 μmol L^{-1} hydrazine and 100 μmol L^{-1} 3,4-dichlorophenol (Fig. 8e), and 25 μmol L^{-1} hydrazine, 100 μmol L^{-1} phenol, and 100 μmol L^{-1} 3,4-dichlorophenol (Fig. 8f). The SWVs of hydrazine in the absence and presence of an interferent are similar (Fig. 8a, c, e, and f), except for a small peak position shift towards positive potentials. The peak potential of hydrazine in the presence of studied interferents remained high enough to determine selectively the hydrazine concentration as the interferent produced negligible amounts of oxidation current and no corresponding peak (Fig. 8b and d). The RSD of the peak heights in Fig. 8a, c, e, and f was 4.70%, close to the RSD for hydrazine-only oxidation at the AuNP-GPE (5.0%). These experiments confirmed that the sensor developed here possessed excellent selectivity toward hydrazine.

3.9. Application

In order to assess the validity of the proposed method for the determination of hydrazine in water samples, two drinking water samples were analyzed under optimum SWV conditions. For the analysis, a 1.0 mL sample of drinking water was diluted to 2 mL with PB (0.2 mol L^{-1}, pH 5). The obtained results showed that no hydrazine was present in either drinking water sample. The recovery was estimated by adding different concentrations of standard hydrazine to the drinking water samples, and the samples were analyzed using the standard addition 'spiking' method. The results are shown in Table 2, and the recoveries were satisfactory and acceptable.

4. Conclusions

This study developed a novel, electroless, linker-free, and extremely straightforward method for preparing AuNP-GPEs for the highly sensitive electrochemical determination of hydrazine concentration. The prepared electrodes showed higher electrocatalytic activities with respect to hydrazine oxidation compared to the bare GPE. The quantification and detection limits of the sensor using the SWV mode were 100 nmol L^{-1} and 42 nmol L^{-1} hydrazine, respectively, whereas the corresponding limits using the amperometry method were 10 μmol L^{-1} and 3.07 μmol L^{-1}, respectively. The AuNP-GPEs displayed reproducible performances, were highly stable, and were not susceptible to interference by common contaminants. Moreover, the AuNP-GPE performed well in the determination of hydrazine concentration in water samples.

Acknowledgments

The authors gratefully acknowledge funding support from King Abdulaziz City for Science and Technology (KACST) through the Science & Technology Unit at King Fahd University of Petroleum & Minerals (KFUPM): Project no. 09-BIO780-04, as part of the National Science, Technology and Innovation Plan.

References

[1] Agency for Toxic Substances and Disease Registry (ATSDR), Toxicological Profile for Hydrazines, U.S. Department of Health and Human Services, Public Health Service, Atlanta, Georgia, 1997, pp. 2–6.
[2] M. Mazloum-Ardakani, H. Rajabi, B.B.F. Mirjalili, H. Beitollahi, A. Akbari, J. Solid State Electrochem. 14 (2010) 2285–2292.
[3] U.S. Environmental Protection Agency. Integrated Risk Information System (IRIS) on Hydrazine/Hydrazine Sulfate. National Center for Environmental Assessment, Office of Research and Development, Washington, DC, 1999.
[4] A.D. Smolenkov, O.A. Shpigun, Talanta 102 (2012) 93–100.
[5] A. Afkhami, A.R. Zarei, Talanta 62 (2004) 559–565.
[6] J. Svitkova, M. Machkova, P. Šatkovska, K. Cinkova, L. Švorc, Acta Chim. Slovaca 5 (2012) 42–46.
[7] S.A. Ozkan, Curr. Pharma. Anal. 5 (2009) 127–143.
[8] A. Ozcan, Y. Sahin, Biosens. Bioelectron. 25 (2010) 2497–2502.
[9] J. Wang, A. Kawde, E. Sahlin, Analyst 125 (2000) 5–7.
[10] W. Gao, J. Song, N. Wu, J. Electroanal. Chem. 576 (2005) 1–7.
[11] G. Hao, D. Zheng, T. Gan, C. Hu, S. Hu, J. Exp. Nanosci. 6 (2011) 13–28.
[12] F.-Y. He, A.-L. Liu, J.-H. Yuan, W.K.T. Coltro, E. Carrilho, X.-H. Xia, Anal. Bioanal. Chem. 382 (2005) 192–197.
[13] Y.-L. Hu, Y. Lu, G.-J.u.n. Zhou, X.-H. Xia, Talanta 74 (2008) 760–765.
[14] Y. Lu, Y.-L. Hu, X.-H. Xia, Talanta 79 (2009) 1270–1275.
[15] U. Chandra, B.E.K. Swamy, O. Gilbert, S. Reddy, B.S. Sherigara, Am. J. Anal. Chem. 2 (2011) 262–269.
[16] Y. Dilgin, B. Kızılkaya, B. Ertek, F. Isık, D.G. Dilgin, Sens. Actuators B 171–172 (2012) 223–229.
[17] C. Zhang, G. Wang, Y. Ji, M. Liu, Y. Feng, Z. Zhang, B. Fang, Sens. Actuators B150 (2010) 247–253.
[18] J. Li, H. Xie, L. Chen, Sens. Actuators B 153 (2011) 239–245.
[19] J. Zhao, M. Zhu, M. Zheng, Y. Tang, Y. Chen, T. Lu, Electrochim. Acta 56 (2011) 4930–4936.
[20] V. Lyutov, V. Tsakova, J. Electroanal. Chem. 661 (2011) 186–191.
[21] F. Zhang, L. Zhang, J. Xing, Y. Tang, Y. Chen, Y. Zhou, T. Lu, X. Xia, ChemPlus Chem. 77 (2012) 914–922.
[22] J. Li, X. Lin, Sens. Actuators B 126 (2007) 527–535.
[23] Z. Yin, L. Liu, Z. Yang, J. Solid State Electrochem. 15 (2011) 821–827.
[24] A. Abbaspour, A. Khajehzadeh, A. Ghaffarinejad, J. Electroanal. Chem. 631 (2009) 52–57.

[25] G. Chang, Y. Luo, W. Lu, J. Hu, F. Liao, X. Sun, Thin Solid Films 519 (2011) 6130–6134.
[26] S.K. Mehta, K. Singh, A. Umar, G.R. Chaudhary, S. Singh, Sci. Adv. Mater. 3 (2011) 962–967.
[27] S. Ameen, M.S. Akhtar, H.S. Shin, Talanta 100 (2012) 377–383.
[28] Y.-Y. Tang, C.-L. Kao, P.-Y. Chen, Anal. Chim. Acta 711 (2012) 32–39.
[29] S. Kesavan, S.B. Revin, S.A. John, J. Mater. Chem. 22 (2012) 17560–17567.
[30] R.N. Goyal, M.A. Aziz, M. Oyama, S. Chatterjee, A.R.S. Rana, Sens. Actuators B 153 (2011) 232–238.
[31] M.A. Aziz, S. Patra, H. Yang, Chem. Commun. (2008) 4607–4609.
[32] M. Behpour, S.M. Ghoreishi, E. Honarmand, Int. J. Electrochem. Sci. 5 (2010) 1922–1933.
[33] S. Mathur, A. Erdem, C. Cavelius, S. Barth, J. Altmayer, Sens. Actuators B 136 (2009) 432–437.
[34] M. Rezaei, S.H. Tabaian, D.F. Haghshenas, Electrochim. Acta 59 (2012) 360–366.
[35] E. Mohammad, M. Norita, Sci. China Chem. 55 (2012) 247–255.
[36] M. Etesami, F.S. Karoonian, N. Mohamed, J. Chin. Chem. Soc. 58 (2011) 688–693.
[37] H.C.B. Kalachar, S. Basavanna, R. Viswanatha, Y.A. Naik, D.A. Raj, P.N. Sudha, Electroanalysis 23 (2011) 1107–1115.
[38] M. Muti, F. Kuralay, A. Erdem, S. Abaci, T. Yumak, A. Sinag, Talanta 82 (2010) 1680–1686.
[39] T. Yumak, F. Kuralay, M. Muti, A. Sinag, A. Erdem, S. Abaci, Colloids Surf. B: Biointerfaces 86 (2011) 397–403.
[40] A.C. Cruickshank, A.J. Downard, Electrochim. Acta 54 (2009) 5566–5570.
[41] S. Patra, J. Das, H. Yang, Electrochim. Acta 54 (2009) 3441–3445.
[42] J. Wang, A. Kawde, Anal. Chim. Acta 431 (2001) 219–224.
[43] D. Andreescu, T.K. Sau, D.V. Goia, J. Colloid Interface Sci. 298 (2006) 742–751.
[44] S. Kumar, S. Zou, J. Phys. Chem. B 109 (2005) 15707–15713.
[45] J.A. Lopez-Sanchez, N. Dimitratos, C. Hammond, G.L. Brett, L. Kesavan, S. White, P. Miedziak, R. Tiruvalam, R.L. Jenkins, A.F. Carley, D. Knight, C. J. Kiely, G.J. Hutchings, Nat. Chem. 3 (2011) 551–556.
[46] C. Engelbrekt, K.H. Sørensen, J. Zhang, A.C. Welinder, P.S. Jensen, J. Ulstrup, J. Mater. Chem. 19 (2009) 7839–7847.
[47] X. Shan, S. Wang, W. Wang, N. Tao, Anal. Chem. 83 (2011) 7394–7399.
[48] H.R. Zare, M.R. Shishehbore, D. Nematollahi, M.S. Tehrani, Sens. Actuators B 151 (2010) 153–161.
[49] H.R. Zare, A.M. Habibirad, J. Solid State Electrochem. 10 (2006) 348–359.
[50] B. Fang, C. Zhang, W. Zhang, G. Wang, Electrochim. Acta 55 (2009) 178–182.
[51] J. Panchompoo, L. Aldous, C. Downing, A. Crossley, R.G. Compton, Electroanalysis 23 (2011) 1568–1578.
[52] L. Shang, F. Zhao, B. Zeng, Electroanalysis 24 (2012) 2380–2386.
[53] J.S. Sophia, S. Devi, K. Pandian, Int. J. Electrochem. Sci. 7 (2012) 6580–6598.
[54] H.R. Zare, Z. Shekari, N. Nasirizadeh, A.A. Jafari, Catal. Sci. Technol. (2012) 2492–2501.